ACS OMEGA

http://pubs.acs.org/journal/acsodf

Article

Study on the Kinetics of Hydration Transformation from Hemihydrate Phosphogypsum to Dihydrate Phosphogypsum in Simulated Wet Process Phosphoric Acid

Bingqi Wang, Lin Yang,* Tong Luo, and Jianxin Cao

Cite This: *ACS Omega* 2021, 6, 7342−7350

Read Online

ACCESS | Metrics & More | Article Recommendations

ABSTRACT: The key technology of wet process phosphoric acid recrystallization is phosphogypsum phase transformation. In this study, the hydration of α-hemihydrate phosphogypsum (α-HH) to dihydrate phosphogypsum (DH) and the influence of process parameters on hydration kinetics are performed by modifying a dispersive kinetic model in the simulation of wet process phosphoric acid recrystallization. Results show that the modified dispersive kinetic model is very important in describing the entire kinetic process, indicating that α-HH−DH hydration includes induction of nucleation and growth restriction. The hydration rate of α-HH−DH substantially accelerates with the decrease of temperature and phosphoric acid concentration because the activation entropy of the reaction increases during the induction stage and the growth stage, which reduces the activation energy barrier. Moreover, the hydration rate of α-HH−DH considerably accelerates with the increase of SO_4^{2-} ion concentration. Activation entropy increases in the induction stage, causing the activation energy barrier to decrease. Activation enthalpy increases in the growth stage, causing the activation energy barrier to decrease. The influence of process parameters on the rate of the α-HH−DH hydration reaction follows the order SO_4^{2-} ion concentration > phosphoric acid concentration > temperature. Therefore, controlling the three parameters of temperature, phosphoric acid concentration, and SO_4^{2-} ion concentration are important for improving the conversion rate of α-HH−DH and the purity of DH products in the production of wet process phosphoric acid.

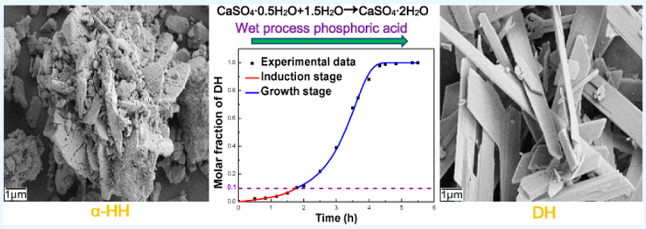

1. INTRODUCTION

Phosphoric acid is a very important chemical intermediate product in the production of phosphate fertilizer, medicine, and food.[1−3] Wet process phosphoric acid can be obtained by decomposing phosphate rock with sulfuric acid, as expressed by eq 1.

$$Ca_5F(PO_4)_3 + 5H_2SO_4 + nH_2O \rightarrow 3H_3PO_4 + 5CaSO_4{\cdot}nH_2O + HF\uparrow \quad (1)$$

According to the different contents of calcium sulfate crystal water obtained in the production, it can be divided into one-step crystallization methods such as dihydrate phosphogypsum (DH), α-hemihydrate phosphogypsum (α-HH), and anhydrous phosphogypsum (AH). Approximately 5 tons of phosphogypsum (PG) is emitted per year for each ton of P_2O_5 produced.[4,5] Statistics shows that about 200−300 million tons of PG is produced annually worldwide.[6] However, the resource utilization rate is less than 15%,[7] and a large amount of PG still uses the method of accumulation and landfilling,[8] which damages the surrounding land and the environment. The recovery rate of P_2O_5 obtained by the one-step process is low, generally only 88−96.5%.[9] In addition, the byproduct PG has a high impurity content and is difficult to utilize as a resource directly. The recrystallization method is to filter and wash the slurry in the one-step process and then place it in the phosphoric acid reaction tank for the secondary transformation of gypsum crystal form.[10] This method can decompose the insoluble P and eutectic P in PG and improve the P_2O_5 recovery rate of phosphate rock as high as 99% or more. Moreover, high-purity PG can be produced by recrystallization, without pretreatment, and can be directly used as a raw material for the production of building materials such as building gypsum, gypsum products, and cement retarders. Therefore, wet process phosphoric acid recrystallization has a great implication for improving the resource utilization rate of PG and environmental protection.[11,12]

The key technology of wet process phosphoric acid recrystallization is PG phase transformation, which mainly

Received: November 6, 2020
Accepted: February 23, 2021
Published: March 8, 2021

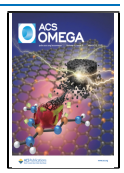

ACS Publications

© 2021 The Authors. Published by American Chemical Society

includes the conversion of DH to α-HH and the conversion of α-HH to DH. The concentration of 33−35% P_2O_5 wet process phosphoric acid is produced by DH−α-HH recrystallization,[13] whereas the concentration of 42−52% P_2O_5 wet process phosphoric acid is produced by α-HH−DH recrystallization.[14] Researchers have concentrated on reporting the phase transformation of $CaSO_4$ in aqueous solutions, salt solutions, and mixed electrolyte of HCl + $CaCl_2$ and the relationship with solubility. Singh et al. introduced the hydration characteristics of α-HH and β-hemihydrate phosphogypsum (β-HH) in aqueous solutions and the influence of chemical additives on crystal growth. Avrami, Schiller, and Ridge kinetic equations were introduced to explain hydration.[15] Hand tested Ridge and Schiller equations through Avrami equations based on numerical calculations and found that these three equations are compatible within certain data ranges.[16] However, Ridge disagreed with Hand's conclusion and believed that Avrami equation has no definite validity in this field.[17] This situation shows that the hydration kinetic equation of hemihydrate calcium sulfate remains controversial. Freyer et al. reviewed the phase diagram of the $CaSO_4$ phase in different electrolyte salt solutions. The difference in the solubility and water activity of the $CaSO_4$ phase in different solutions led to the uncertainty of the dehydration conversion temperature of DH−AH and DH−HH.[18] Li et al. studied the solubility of the $CaSO_4$ phase in pure HCl medium and HCl + $CaCl_2$ mixed medium from 283 to 353 K and found that the solubility of DH, HH, and AH changed greatly due to changes in the solution medium.[19] Afterward, Fu et al. used thermogravimetric and differential scanning calorimetry (TG-DSC) to study the conversion kinetics of DH−α-HH in $CaCl_2$ solutions. They found that the dehydration conversion of DH−α-HH in $CaCl_2$ solutions can use a relatively general dispersive kinetic model to describe the conversion of DH−α-HH.[20] The dispersive kinetic model is suitable for studying asymmetric heterogeneous transformation. It connects the activation enthalpy with the thermodynamic component and the activation entropy with the dynamic component through two parameters, namely, α and β. Thus, it can explain the $CaSO_4$ phase transformation well.[21,22] However, this kinetic model is only applicable to the situation where the phase conversion rate of $CaSO_4$ reaches 100%.

In the production of wet process phosphoric acid, the phase conversion of $CaSO_4$ cannot achieve a complete conversion due to the influence of SO_4^{2-} ion concentration, production time, and other factors. Grzmil et al. studied the influence of temperature, phosphoric acid concentration, SO_4^{2-} ion concentration, and α-HH crystal nucleus on the conversion of DH−α-HH in wet process phosphoric acid. The results showed that increasing temperature, phosphoric acid concentration, and adding α-HH nucleus can substantially increase the degree of DH−α-HH conversion, but the conversion is not complete, and the highest conversion rate is only 97.7%.[23] Moreover, wet process phosphoric acid is different from other solutions such as aqueous solutions or salt solutions. The water activity of the reaction system and the solubility of the $CaSO_4$ phase vary, resulting in a change in supersaturation. Furthermore, the hydration of α-HH−DH shows different thermal and hydration characteristics. The direct use of the dispersive kinetic model produces large errors, and comparing the degree of influence of the process parameters on the phase transformation of $CaSO_4$ is difficult. Therefore, this article analyzes kinetics of hydration conversion of α-HH−DH in the medium of wet process phosphoric acid in order to obtain a modified dispersive kinetic model that achieves a good agreement in α-HH−DH hydration process. On this basis, the influence of temperature, phosphoric acid concentration, and SO_4^{2-} ion concentration on the hydration kinetics of α-HH−DH is discussed in depth, which provides a theoretical basis for wet process phosphoric acid recrystallization.

2. RESULTS AND DISCUSSION

2.1. α-HH−DH Hydration Thermodynamic Analysis and Conversion. The hydration of α-HH−DH is expressed by eq 2.

$$CaSO_4{\cdot}0.5H_2O + 1.5H_2O \rightarrow CaSO_4{\cdot}2H_2O \quad (2)$$

The enthalpy change (Δ*H*), entropy change (Δ*S*), Gibbs free energy change (Δ*G*), and equilibrium constant (expressed in log *K*) of α-HH−DH hydration conversion at 50−70 °C were calculated by the HSC Chemistry software, as shown in Table 1.

Table 1. Δ*H*, Δ*S*, Δ*G*, and log *K* of α-HH−DH Hydration Conversion at 50−70 °C

T (°C)	Δ*H* (kJ)	Δ*S* (J/K)	Δ*G* (kJ)	log *K*
50	−18.215	−44.777	−3.746	0.606
60	−18.619	−46.006	−3.292	0.516
70	−19.007	−47.156	−2.826	0.430

Table 1 shows that the hydration of α-HH−DH is an exothermic reaction. Δ*G* < 0 indicates that the reaction proceeds spontaneously. The log *K* decreases as the temperature increases, indicating that the degree of reaction progress decreases as the temperature increases.

At 60 °C with 30.0% P_2O_5 phosphoric acid solution, the morphology evolution of the solid during the hydration of α-HH−DH was studied by scanning electron microscopy (SEM), and the results are shown in Figure 1. The X-ray diffraction (XRD) analysis method was used to identify the phase, and the results are shown in Figure 2. TG-DSC was used to analyze the hydration of α-HH−DH, and the results are shown in Figure 3.

Figure 1a,b shows that α-HH presents irregularly shaped spherical polycrystals, and DH crystals with plate-like morphology are not observed. Figure 1c shows that DH crystals with plate-like morphology are wrapped together. Figure 1d shows that most of the plate-like DH crystals form and several honeycomb-like crystals can be clearly seen. This is because dissolution of α-HH starts from the edge part of the particles, thus small depressions (etching) form on the surface, and then DH crystals generate near the honeycomb-like crystals in the preaccelerated period of α-HH−DH conversion.[24] Figure 1e shows that a large number of plate-like DH crystals form and α-HH crystals are almost invisible. The crystals' surface is not smooth and has cracks possibly because the newly formed DH crystals have not fully grown. Figure 1f shows that DH crystals have a relatively regular plate-like morphology, a smooth surface, and a good crystallinity. The microscopic morphology of the 0−5 h transformation can clearly show α-HH crystals slowly dissolving and DH crystals recrystallizing and nucleating. This observation proves that the transformation of α-HH−DH follows the mechanism of dissolution and recrystallization.

Figure 2 shows that, during conversion, the diffraction peak intensity of α-HH gradually decreases until it disappears, and

https://dx.doi.org/10.1021/acsomega.0c05432
ACS Omega 2021, 6, 7342−7350

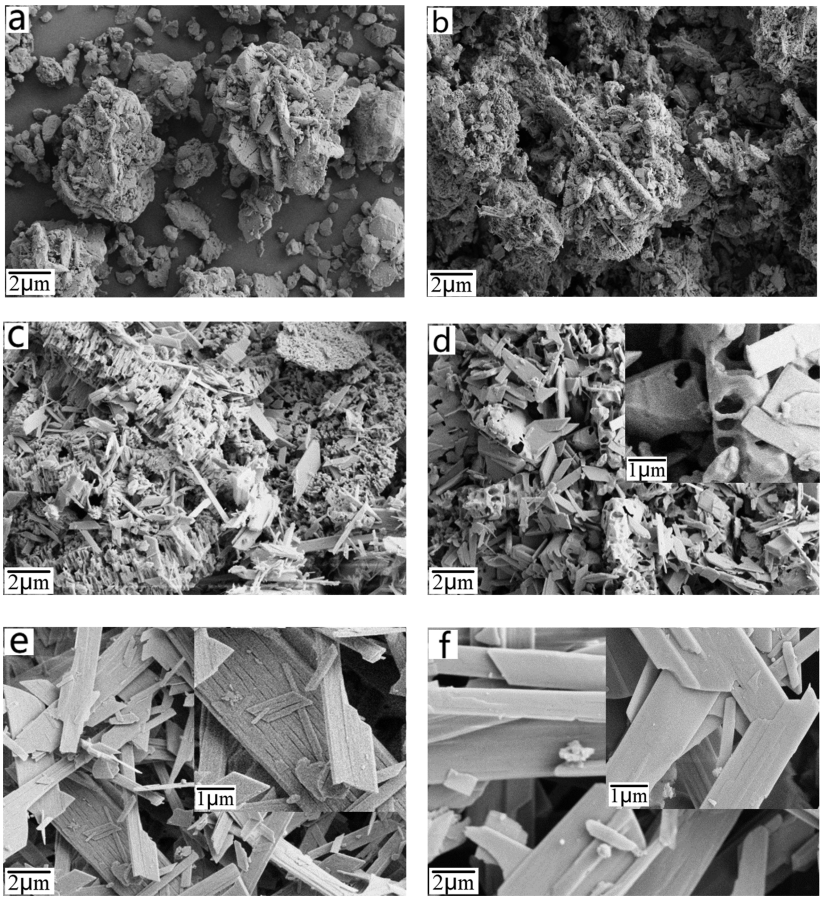

Figure 1. SEM images of the morphology evolution of the solid at 0 h (a), 1 h (b), 2 h (c), 3 h (d), 4 h (e), and 5 h (f) during the hydration of α-HH−DH.

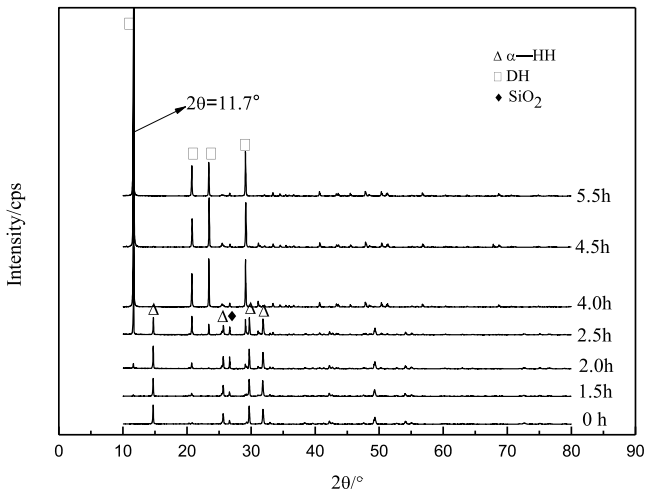

Figure 2. XRD pattern of α-HH−DH with different conversion times.

the diffraction peak intensity of DH gradually increases. Almost no diffraction peak of DH is observed at 0 and 1.5 h, especially at $2\theta = 11.7°$. The DH diffraction peak begins to appear at 2 h. The DH diffraction peak increases rapidly from 2.5 to 4 h and stabilizes after 4 h. The experimental data obtained by measuring the crystal water are consistent, which proves the reliability of the experimental method.

Figure 3 shows the TG-DSC curves of α-HH−DH conversion. The TG curves show that the weight loss of the solid phase continuously increases as the conversion time increases. When the conversion time is 2 h, the weight loss of TG data is 8.59%. At the same time, the crystal water content of the sample at the conversion time of 2 h is 8.56% using the Gypsum Chemical Analysis Method, which is consistent with the TG data. The DSC curve at the conversion time of 2 h shows only one endothermic peak at 149.2 °C, indicating that it is mainly composed of α-HH at this time. The DSC curves present two endothermic peaks at the conversion time from 3.0 to 6.0 h, which shows that the first endothermic peak at 138.9 °C slowly expands and the second endothermic peak at 149.2 °C slowly shrinks as the conversion time increases. The first endothermic peak indicates that DH loses 1.5 H_2O to become α-HH, and the second endothermic peak indicates that α-HH loses 0.5 H_2O to become AH. The two endothermic peaks gradually stabilize at the conversion time from 4 to 6 h.

2.2. α-HH−DH Hydration Driving Force and Kinetic Equation. During the hydration of α-HH−DH in 60 °C, 30.0% P_2O_5 phosphoric acid solution, and in 60 °C, 5% SO_4^{2-} ion concentration, 30.0% P_2O_5 phosphoric acid solution, the changes of Ca^{2+} ion concentration at the dissolution equilibrium and DH mole fraction with different times are shown in Figure 4.

The supersaturation of DH nucleation and growth is expressed by eq 3.[20]

https://dx.doi.org/10.1021/acsomega.0c05432
ACS Omega 2021, 6, 7342−7350

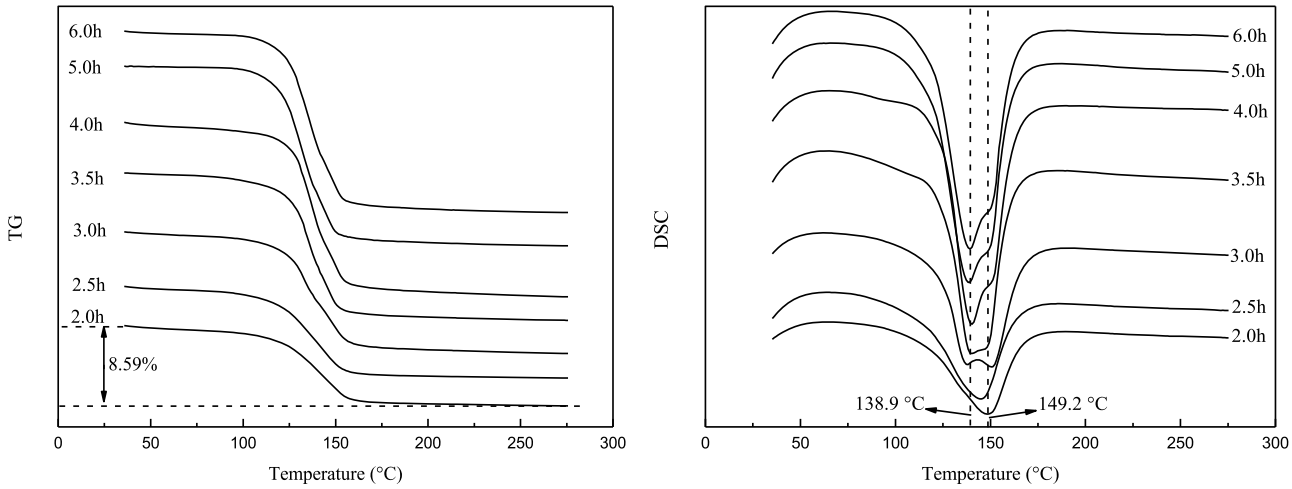

Figure 3. TG-DSC charts of α-HH−DH with different conversion times.

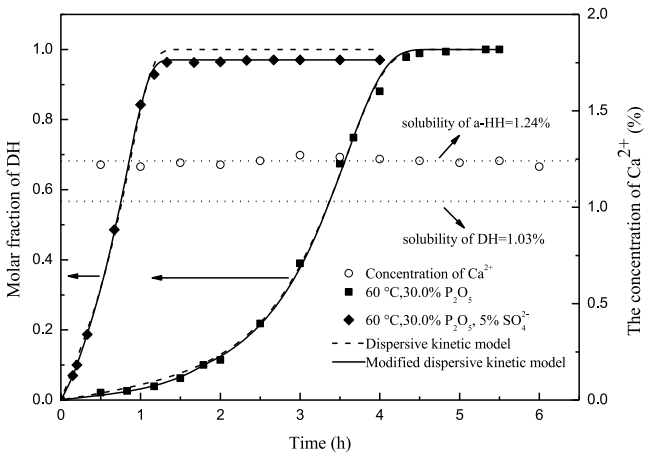

Figure 4. Changes of Ca^{2+} ion concentration and DH mole fraction with different times during the hydration of α-HH−DH.

$$S_{DH} = \frac{C_{e,HH}}{C_{e,DH}} = \frac{m(Ca^{2+})_{HH}}{m(Ca^{2+})_{DH}} = \frac{K_{sp,HH}/\{\gamma(Ca^{2+})\gamma(SO_4^{2-})m(SO_4^{2-})a_w^{0.5}\}}{K_{sp,DH}/\{\gamma(Ca^{2+})\gamma(SO_4^{2-})m(SO_4^{2-})a_w^{2}\}} = \frac{K_{sp,HH}a_w^{1.5}}{K_{sp,DH}} \quad (3)$$

where $C_{e,DH}$ and $C_{e,HH}$ are the solubility of DH and α-HH, respectively. $m(Ca^{2+})$ and $m(SO_4^{2-})$ are the molar concentrations of Ca^{2+} and SO_4^{2-} ions in the solution, respectively. $K_{sp,DH}$ and $K_{sp,HH}$ are the solubility product constants of DH and α-HH, respectively. $\gamma(Ca^{2+})$ and $\gamma(SO_4^{2-})$ are the ion activity coefficients, and a_w is the water activity.

The dotted line in Figure 4 shows that the solubility of α-HH (1.24%) is greater than the solubility of DH (1.03%). Ca^{2+} ion concentration in the solution fluctuates around the solubility of α-HH, indicating that the driving force of α-HH−DH conversion is the difference in solubility between the two, which leads to increased supersaturation. Equation 3 shows that the supersaturation of DH nucleation is affected by the solubility product ratio of α-HH to DH ($K_{sp,HH}/K_{sp,DH}$) as well as water activity.

The dispersive kinetic model is shown in eq 4.

$$y = 1 - \exp\left\{-\frac{\alpha}{t}[\exp(\beta t^2) - 1]\right\} \quad (4)$$

where y is the mole fraction of the product, t is the conversion time, α (h) is an activation enthalpy parameter independent of time, and β (h^{-2}) is a time-varying parameter related to activation entropy.

Values of α and β are expressed in eqs 5 and 6.

$$\alpha = A^{n-1}e^2e^{-E_a^0/RT} = A^{n-1}e^{-\Delta H^*/RT} \quad (5)$$

$$\beta = \frac{\Delta S^*}{Rt^2} \quad (6)$$

where A is the Arrhenius constant, n is the constant related to the dimensionality of the system that is assumed to be 0, ΔH^* is the activation enthalpy, ΔS^* is the activation entropy, E_a^0 is the total for the time-independent part of the activation energy, and R is the gas constant.[22]

The activation energy barrier is the difference between the ground state and the active state Gibbs free energy, which is represented by eq 7.[22]

$$E_a = E_a^0 - RT\beta t^2 \quad (7)$$

The dispersive kinetic model was used to fit the DH mole fraction variation curve with time, as shown by the dashed line in Figure 4. In 60 °C, 30.0% P_2O_5 phosphoric acid solution, α = 0.1477 h, β = 0.2644 h^{-2}, and R^2 = 0.9988. In 60 °C, 30.0% P_2O_5 phosphoric acid solution, 5% SO_4^{2-} ion concentration, α = 0.3307 h, β = 1.8397 h^{-2}, and R^2 = 0.9947. Moreover, in 60 °C, 30.0% P_2O_5 phosphoric acid solution, 5% SO_4^{2-} ion concentration, the end of the curve is 100%. However, the experimental data show that the conversion rate can only reach 97%, and the conversion of α-HH−DH under this condition is not complete. The analysis of eq 4 shows that when t approaches positive infinity, y is 100%, which means that only the case where the conversion rate is 100% can be fitted. The conversion is complete in the 30.0% P_2O_5 phosphoric acid solution at 60 °C, but the fitting curve deviates greatly from the experimental data at 0.83, 1.17, and 1.50 h, indicating that the dispersive kinetic equation cannot accurately reflect the conversion in the early stages.

https://dx.doi.org/10.1021/acsomega.0c05432
ACS Omega 2021, 6, 7342−7350

The α-HH−DH hydration was divided into two stages to modify the dispersive kinetic equation. The first is the induction stage, which refers to the mole fraction of the product $0 \leq y \leq 10\%$, and the corresponding time is called the induction time.[25] The second is the growth stage, which refers to the mole fraction of the product $y > 10\%$. The growth rate is defined as the change in mole fraction of DH per unit of time in the second stage. For wet process phosphoric acid media, a more universally applicable kinetic equation in the hydration of α-HH−DH is shown in eq 8, which is applicable to complete conversion and incomplete conversion.

$$y = \begin{cases} 1 - \exp\left\{-\frac{\alpha}{t}[\exp(\beta t^2) - 1]\right\} & (0 \leq t \leq t_{\text{ind}}) \\ y_{\max} - \exp\left\{-\frac{\alpha}{t}[\exp(\beta t^2) - 1]\right\} & (t > t_{\text{ind}}) \end{cases} \quad (8)$$

where t_{ind} is the induction time and $y_{\max}$ is the maximum mole fraction of the product.

The curve of the mole fraction of DH over time was fitted by eq 8, as shown by the solid line in Figure 4. In 60 °C, 30.0% P_2O_5 phosphoric acid solution, in the induction stage, α = 5.5900 h, β = 0.4610 h^{-2}, and R^2 = 0.9968. In the growth stage, α = 0.1370 h, β = 0.2700 h^{-2}, and R^2 = 0.9993. In 60 °C, 30.0% P_2O_5 phosphoric acid solution, 5% SO_4^{2-} ion concentration, in the induction stage, α = 0.0469 h, β = 9.2800 h^{-2}, and R^2 = 1.0000. In the growth stage, α = 0.3510 h, β = 1.9100 h^{-2}, and R^2 = 0.9999.

The results of the fitting show that the accuracy is much improved, and the fitting curve is closer to the experimental data. In the wet process phosphoric acid medium, kinetic parameters α and β vary at different stages in the conversion of α-HH−DH. α and β are functions of activation enthalpy and activation entropy in thermodynamics, respectively. Equation 7 shows that activation energy barrier (E_a) is affected by α and β. In the induction stage and the growth stage, parameters α and β vary, and the thermochemical characteristics of the reaction are different. The activation energy barrier varies, causing the driving force and the conversion rate to change.

In 60 °C, 30.0% P_2O_5 phosphoric acid solution, combined with the experimental data and the fitting curve, DH is in the slow growth stage within 1.8 h of the crystallization induction period. At this time, $CaSO_4$ mainly exists in the form of α-HH, and the XRD pattern and the TG-DSC curves are consistent. The conversion rate of α-HH−DH is considerably accelerated, and the mole fraction of DH reaches 98% in 4.3 h due to the change of driving force during the growth stage. At this time, $CaSO_4$ mainly exists in the form of DH. Over time, the conversion is complete. It shows that the hydration of α-HH−DH is at the cost of the disappearance of α-HH in wet process phosphoric acid medium, which is a process of inducing nucleation and growth restriction.

2.3. Influence of Process Parameters on the Hydration Kinetics of α-HH−DH. *2.3.1. Temperature.* Based on 55−65 °C, 30.0% P_2O_5 concentration, the changes of DH mole fraction with different times are shown in Figure 5.

Figure 5 shows that conversion speeds up remarkably as temperature decreases. When temperature decreases from 65 to 55 °C, the time required to complete the conversion of α-HH−DH is shortened from 5 to 4 h. The steam balance method was used to measure water activity.[26] $K_{sp,DH}$ and $K_{sp,HH}$ were calculated according to the formula.[27] From eq 3,

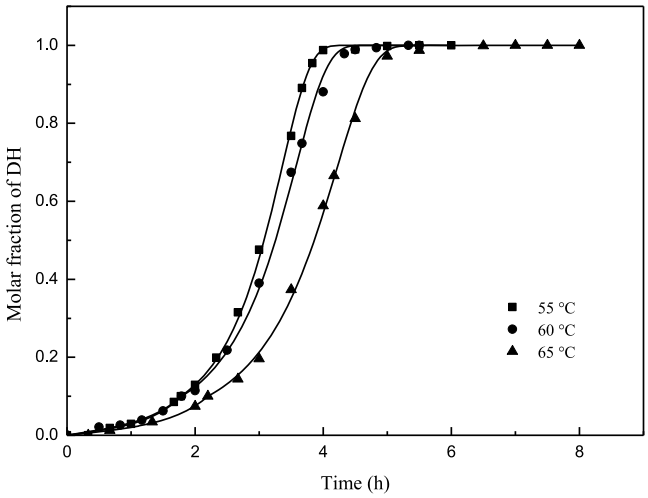

Figure 5. Changes of DH molar fraction with different times in 30.0% P_2O_5 phosphoric acid solution at 55−65 °C.

supersaturation (S_{DH}) can be calculated, and induction time (t_{ind}) and growth rate (v) were obtained, as shown in Figure 5. Under 55−65 °C, 30.0% P_2O_5 concentration, the kinetic parameters of α-HH−DH conversion, t_{ind}, v, a_w, $K_{sp,DH}$, $K_{sp,HH}$, and S_{DH} are listed in Table 2.

Table 2 shows that in 30.0% P_2O_5 phosphoric acid solution, as temperature increases from 55 to 65 °C, parameter α increases from 0.0408 to 0.0456 and parameter β decreases from 0.5440 to 0.3730 during the induction stage. In the growth stage, parameter α increases from 0.1054 to 0.1410 and parameter β decreases from 0.3230 to 0.2010. Combining eqs 5, 6, and 7 shows that parameter α increases; the corresponding ΔH^* or E_a^0 decreases, and E_a decreases. Parameter β decreases, indicating that ΔS^* decreases and E_a increases. When the temperature increases, whether in the induction stage or the growth stage, the changes in parameter β are greater than that in parameter α. Thus, ΔS^* decreases, leading E_a to increase, and then reaction rate slows down.

Table 2 shows that in 30.0% P_2O_5 phosphoric acid solution, temperature decreases from 65 to 55 °C; induction time is shortened from 2.18 to 1.78 h, and the corresponding growth rate increases from 0.29 to 0.37. The water activity is 0.68 at different temperatures, and the solubility product ratio of α-HH to DH increases from 1.97 at 65 °C to 2.32 at 55 °C, resulting in an increase in supersaturation from 1.11 to 1.30. The findings show that supersaturation increases with the increase of solubility product ratio of α-HH to DH, thereby promoting the conversion of α-HH−DH.

2.3.2. Phosphoric Acid Concentration. Changes of DH molar fraction with different times in 25.0−32.5% P_2O_5 phosphoric acid solution at 60 °C are shown in Figure 6.

Figure 6 shows that at 60 °C, as phosphoric acid concentration decreases from 32.5% P_2O_5 to 25.0% P_2O_5, the time required to complete the conversion of α-HH−DH decreases from 8 to 2 h. The kinetic parameters of α-HH−DH conversion, t_{ind}, v, a_w, and S_{DH} at 60 °C and 25.0−32.5% P_2O_5 concentration are listed in Table 3.

Table 3 shows that at 60 °C, as the phosphoric acid concentration increases from 25.0% P_2O_5 to 32.5% P_2O_5, parameter α increases from 0.0343 to 0.1120 and parameter β decreases from 2.5000 to 0.1190 during the induction stage. However, parameter α increases from 0.0996 to 0.2280, and

https://dx.doi.org/10.1021/acsomega.0c05432
ACS Omega 2021, 6, 7342−7350

Table 2. Kinetic Parameters, t_{ind}, v, a_w, $K_{sp,DH}$, $K_{sp,HH}$, and S_{DH} of α-HH−DH Conversion in 30.0% P_2O_5 Phosphoric Acid Solution at 55−65 °C

T (°C)	period	α (h)	β (h^{-2})	R^2	t_{ind} (h)	v (h^{-1})	a_w	$K_{sp,DH}$ ($\times 10^5$)	$K_{sp,HH}$ ($\times 10^5$)	S_{DH}
55	induction stage	0.0408	0.5440	0.9975	1.78		0.68	2.80	6.49	1.30
	growth stage	0.1054	0.3230	0.9998		0.37				
60	induction stage	0.0559	0.4610	0.9968	1.79		0.68	2.65	5.68	1.20
	growth stage	0.1370	0.2700	0.9993		0.33				
65	induction stage	0.0456	0.3730	0.9985	2.18		0.68	2.50	4.93	1.11
	growth stage	0.1410	0.2010	0.9996		0.29				

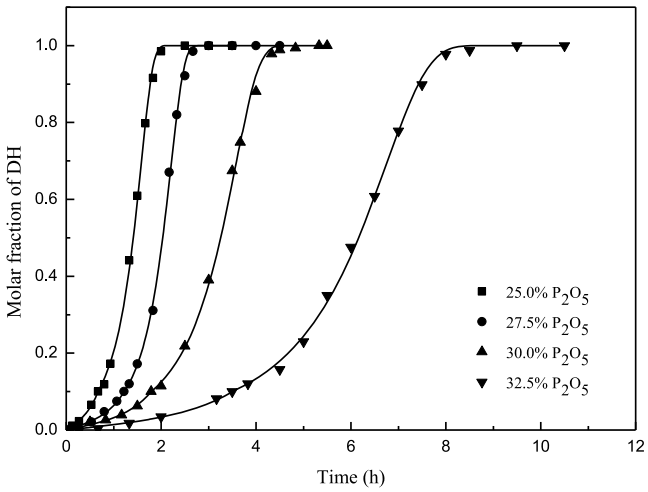

Figure 6. Changes of DH molar fraction with different times in 25.0−32.5% P_2O_5 phosphoric acid solution at 60 °C.

parameter β decreases from 1.1900 to 0.0786 in the growth stage. The above data show that, with the increase of phosphoric acid concentration, in the induction stage and the growth stage, parameter β has a larger variation range than parameter α, which decreases ΔS^*, causing E_a to increase and reaction rate to slow down.

Table 3 shows that at 60 °C, as phosphoric acid concentration decreases from 32.5% P_2O_5 to 25.0% P_2O_5, induction time is shortened from 3.54 to 0.66 h, and growth rate increases substantially from 0.18 to 0.63. The solubility product constants are a function of temperature. At 60 °C, the solubility product ratio of α-HH to DH is 2.14 at different phosphoric acid concentrations, and water activity increases from 0.63 to 0.78 with the decrease of phosphoric acid concentration, resulting in an increase in supersaturation from 1.07 to 1.48. Therefore, the supersaturation of DH nucleation and growth can be increased by reducing phosphoric acid concentration, thereby promoting α-HH−DH transformation.

2.3.3. SO_4^{2-} Ion Concentration. Changes of DH mole fraction with different times under different SO_4^{2-} ion concentration are shown in Figure 7.

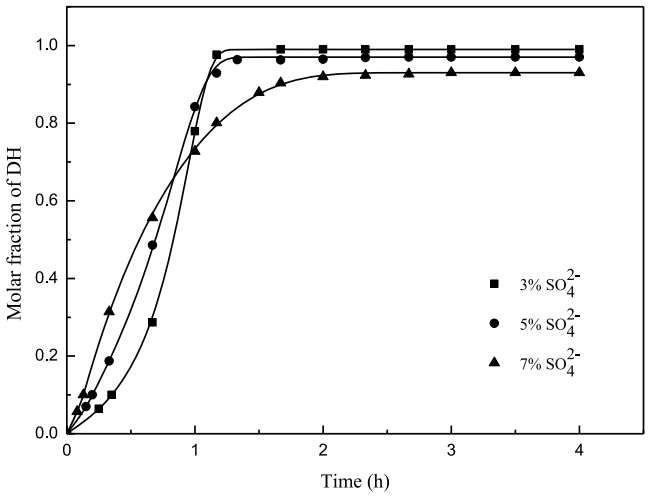

Figure 7. Changes of DH mole fraction with different times in 3−7% SO_4^{2-} ion concentration, 30.0% P_2O_5 phosphoric acid solution at 60 °C.

Figure 7 shows that the presence of SO_4^{2-} ions considerably shortens conversion time, and α-HH−DH conversion is completed in only 1.3 h in the presence of 3% SO_4^{2-} ion concentration. At 0−0.82 h, reaction rate is fast with the increase of SO_4^{2-} ion concentration. Over time, the high concentration of SO_4^{2-} ion inhibits the progress of the reaction, resulting in incomplete conversion. At 60 °C, 30.0% P_2O_5 phosphoric acid solution, 3−7% SO_4^{2-} ion concentration, the kinetic parameters of α-HH−DH transformation induction stage and growth stage, t_{ind}, v, a_w, and S_{DH} are listed in Table 4.

Table 4 shows that in 30.0% P_2O_5 phosphoric acid solution at 60 °C, when the SO_4^{2-} ion concentration increases from 3

Table 3. Kinetic Parameters, t_{ind}, v, a_w, and S_{DH} of α-HH−DH Conversion in 25.0−32.5% P_2O_5 Phosphoric Acid Solution at 60 °C

P_2O_5 (%)	period	α (h)	β (h^{-2})	R^2	t_{ind} (h)	v (h^{-1})	a_w	S_{DH}
25.0	induction stage	0.0343	2.5000	0.9987	0.66		0.78	1.48
	growth stage	0.0996	1.1900	0.9996		0.63		
27.5	induction stage	0.0427	0.9340	0.9961	1.25		0.73	1.34
	growth stage	0.0587	0.7790	0.9996		0.58		
30.0	induction stage	0.0559	0.4610	0.9968	1.79		0.68	1.20
	growth stage	0.1370	0.2700	0.9993		0.33		
32.5	induction stage	0.1120	0.1190	0.9981	3.54		0.63	1.07
	growth stage	0.2280	0.0786	0.9995		0.18		

https://dx.doi.org/10.1021/acsomega.0c05432
ACS Omega 2021, 6, 7342−7350

Table 4. Kinetic Parameters, t_{ind}, v, a_w, and S_{DH} of α-HH−DH Conversion in 3−7% SO_4^{2-} Ion Concentration, 30.0% P_2O_5 Phosphoric Acid Solution at 60 °C

SO_4^{2-} (%)	period	α (h)	β (h^{-2})	R^2	t_{ind} (h)	v (h^{-1})	a_w	S_{DH}
3	induction stage	0.0574	4.0500	1.0000	0.35		0.81	1.56
	growth stage	0.0992	2.8100	0.9999		0.97		
5	induction stage	0.0469	9.2800	1.0000	0.14		0.85	1.68
	growth stage	0.3510	1.9100	0.9999		0.40		
7	induction stage	0.0377	18.3000	1.0000	0.07		0.89	1.80
	growth stage	5.5800	0.2570	0.9999		0.28		

Table 5. Chemical Composition of Hemihydrate Phosphogypsum

compounds	CaO	S	SiO_2	Fe_2O_3	Al_2O_3	MgO	F	K_2O	Na_2O	total P_2O_5	crystal water
% weight	50.69	30.91	5.79	0.31	0.60	0.21	0.79	0.14	0.74	1.66	6.18

to 7% during the induction stage, parameter α decreases from 0.0574 to 0.0377 and parameter β increases from 4.0500 to 18.3000. β has a larger variation range than parameter α, causing E_a to decrease and reaction rate to increase. In the growth stage, parameter α increases from 0.0992 to 5.5800 and parameter β decreases from 2.8100 to 0.2570. E_a decreases, and reaction rate increases because parameter α has a variation range larger than that of parameter β. As SO_4^{2-} ion concentration increases, the reaction rate in the induction stage and the growth stage is accelerated, but the influencing factors in various stages are different. ΔS^* increases in the induction stage, causing E_a to decrease, whereas ΔH^* increases in the growth stage, causing E_a to decrease.

Table 4 shows that in 30.0% P_2O_5 phosphoric acid solution at 60 °C, when SO_4^{2-} ion concentration increases from 3 to 7%, induction time decreases remarkably from 0.35 to 0.07 h, and water activity increases from 0.81 to 0.89. This is because SO_4^{2-} ions increase the supersaturation of DH from 1.56 to 1.80, indicating that the SO_4^{2-} ion promotes α-HH−DH conversion. However, growth rate is reduced, resulting from a large number of DH fine flake particles attached to the surface of the α-HH crystals, preventing further transformation of α-HH. Passivation occurs in the system,[28] leading to a slow growth rate of DH and incomplete conversion.

The effects of process parameters on the hydration of α-HH−DH can be detected by comparing the kinetic parameters with the variation in the growth stage. Under the influence of temperature, parameter β decreases from 0.3230 to 0.2010. Under the influence of phosphoric acid concentration, parameter β decreases from 1.1900 to 0.0786. Under the influence of SO_4^{2-} ion concentration, parameter α increases from 0.0992 to 5.5800. These findings show that temperature and phosphoric acid concentration have a large variation range of parameter β during the growth stage, whereas the SO_4^{2-} ion concentration has a large variation range of parameter α during the growth stage. Thus, the influence of process parameters on the hydration of α-HH−DH follows the order SO_4^{2-} ion concentration > phosphoric acid concentration > temperature in the simulated hemihydrate−dihydrate two-step wet process phosphoric acid production.

3. CONCLUSIONS

In this paper, the hydration kinetics of α-HH−DH and the influence of parameters on hydration are studied under the conditions of wet process phosphoric acid by using the kinetic equation to fit the experimental data. The following conclusions are drawn:

(1) The dispersive kinetic model is modified, and the α-HH−DH hydration kinetic process under different parameters is fitted through the form of a piecewise function. The segmented dispersive kinetic model can accurately describe the induction stage and the growth stage of the reaction, considering complete conversion and incomplete conversion, and is more universal. The curve after fitting shows that α-HH−DH hydration includes induction of nucleation and growth restriction.

(2) The hydration rate of α-HH−DH increases considerably with the decrease of temperature and phosphoric acid concentration because ΔS^* increases during the induction and growth stages, causing E_a to decrease. The hydration rate of α-HH−DH also remarkably accelerates with the increase of SO_4^{2-} ion concentration. ΔS^* increases in the induction stage, causing E_a to decrease, whereas ΔH^* increases in the growth stage, causing E_a to decrease. However, over time, reaction rate decreases, and conversion is incomplete because a large number of DH crystals wrap the α-HH.

(3) The influence of process parameters on the rate of α-HH hydration reaction follows the order SO_4^{2-} ion concentration > phosphoric acid concentration > temperature. SO_4^{2-} ion concentration and phosphoric acid concentration mainly affect water activity, and temperature mainly affects solubility product constants. These findings show that if the reaction medium is different, the change of water activity has a great effect on the hydration of α-HH−DH. By reducing temperature and phosphoric acid concentration and increasing SO_4^{2-} ion concentration, the solubility product ratio of α-HH to DH and the water activity increase, thereby increasing the supersaturation of DH and promoting the conversion of α-HH−DH.

4. MATERIALS AND METHODS

4.1. Experimental Materials. α-Hemihydrate phosphogypsum (taken from a phosphorus chemical company in Guizhou) and its chemical composition analysis are shown in Table 5.

Phosphoric acid (85 wt % P_2O_5), sulfuric acid (98 wt % H_2SO_4), and absolute ethanol are all analytical reagents. The experimental water is deionized water.

4.2. Experimental Methods. α-HH−DH hydration experiments were carried out in 25.0−32.5% P_2O_5 phosphoric acid solution at 55−65 °C. The solution was transferred into a three-necked flask reactor with a condenser on the top of the

https://dx.doi.org/10.1021/acsomega.0c05432
ACS Omega 2021, 6, 7342−7350

reactor tube and a Teflon impeller. A thermometer was inserted into the reactor to record the temperature, and glycerol was used to heat and keep the required temperature within ±0.2 °C. A certain amount of α-hemihydrate phosphogypsum was added at a liquid−solid ratio of 4:1 and stirred at a certain speed. During this period, the slurry was extracted at a certain time interval and filtered quickly. The filtrate was measured using a flame atomic absorption spectrophotometer (AA-6300, Shimadzu, Japan) to determine the Ca^{2+} ion concentration. The filter cake was repeatedly washed with hot water until it was neutral, rinsed once with absolute ethanol, and placed in an oven at 50 ± 1 °C to dry to constant weight.

The mole fraction y of DH in the filter cake is shown in eq 9.

$$y = \frac{w_1}{w_1 + w_2} \times 100\% \tag{9}$$

where w_1 and w_2 are the contents of DH and α-HH, respectively, which can be calculated from the content of crystal water in the sample (refer to GB/T5484-2012 Gypsum Chemical Analysis Method), as shown in eqs 10 and 11.

$$M_1 w_1 + M_2 w_2 = m_1 \tag{10}$$

$$(2w_1 + 0.5w_2) \times 18 = m_1 - m_2 \tag{11}$$

where M_1 is the molar mass of DH, M_2 is the molar mass of α-HH, m_1 is the initial mass of the sample, and m_2 is the mass of the sample after dehydration.

The sample was treated with gold spray, and microscopic morphology was studied by a scanning electron microscope (Zeiss ∑IGMA, Germany). An X-ray diffractometer (PANalytical Holland) was used to analyze the composition of the solid phase. The test conditions were as follows: Cu target, voltage of 40 kV, current of 40 mA, continuous scanning, scanning speed of 10°/min, and scanning range of 2θ: 10−80°. TG-DSC (STA449F3, NET-ZSCH, Germany) analysis methods were verified. For TG-DSC measurement, about 5 mg of solids was sealed in a covered Al_2O_3 crucible and scanned at a rate of 10 °C/min under a N_2 gas atmosphere.

AUTHOR INFORMATION

Corresponding Author

Lin Yang − *School of Chemistry and Chemical Engineering, Guizhou University, Guiyang 550025, China; Guizhou Engineering Research Center for High Efficiency Utilization of Industrial Waste, Guiyang 550025, China;* orcid.org/0000-0002-5229-3058; Email: ce.lyang@gzu.edu.cn

Authors

Bingqi Wang − *School of Chemistry and Chemical Engineering, Guizhou University, Guiyang 550025, China; Guizhou Engineering Research Center for High Efficiency Utilization of Industrial Waste, Guiyang 550025, China*

Tong Luo − *School of Chemistry and Chemical Engineering, Guizhou University, Guiyang 550025, China; Guizhou Engineering Research Center for High Efficiency Utilization of Industrial Waste, Guiyang 550025, China*

Jianxin Cao − *School of Chemistry and Chemical Engineering, Guizhou University, Guiyang 550025, China; Guizhou Key Laboratory for Green Chemical and Clean Energy Technology, Guiyang 550025, China*

Complete contact information is available at: https://pubs.acs.org/10.1021/acsomega.0c05432

Notes

The authors declare no competing financial interest.

ACKNOWLEDGMENTS

The present work was financially supported by the National Key Research and Development Program (2018YFC1900206), the Scientific and Technological Project of Guizhou Province (2018)2194, and Talent Project Plan of Guizhou Province (2019)5668, (2019)5409, and (2017)5711.

REFERENCES

(1) Ye, C.; Li, J. Wet process phosphoric acid purification by solvent extraction using N-octanol and tributylphosphate mixtures. *J. Chem. Technol. Biotechnol.* **2013**, *88*, 1715−1720.

(2) Hannachi, A.; Habaili, D.; Chtara, C.; Ratel, A. Purification of wet process phosphoric acid by solvent extraction with TBP and MIBK mixture. *Sep. Purif. Technol.* **2007**, *55*, 212−216.

(3) Aznar, M.; Araújo, R. N.; Romanato, J. F.; Santos, G.; d'Ávila, S. G. Salt effects on liquid-liquid equilibrium in water + ethanol + alcohol + salt systems. *J. Chem. Eng. Data* **2000**, *45*, 1055−1059.

(4) Contreras, M.; Pérez-López, R.; Gázquez, M. J.; Morales-Flórez, V.; Santos, A.; Esquivias, L.; Bolívar, J. P. Fractionation and fluxes of metals and radionuclides during the recycling process of phosphogypsum wastes applied to mineral CO_2 sequestration. *Waste Manage.* **2015**, *45*, 412−419.

(5) Rashad, A. M. Phosphogypsum as a construction material. *J. Cleaner Prod.* **2017**, *166*, 732−743.

(6) Pérez-López, R.; Macías, F.; Cánovas, C. R.; Sarmiento, A. M.; Pérez-Moreno, S. M. Pollutant flows from a phosphogypsum disposal area to an estuarine environment: an insight from geochemical signatures. *Sci. Total Environ.* **2016**, *553*, 42−51.

(7) Hentati, O.; Abrantes, N.; Caetano, A. L.; Bouguerra, S.; Gonçalves, F.; Römbke, J.; Pereira, R. Phosphogypsum as a soil fertilizer: ecotoxicity of amended soil and elutriates to bacteria, invertebrates, algae and plants. *J. Hazard. Mater.* **2015**, *294*, 80−89.

(8) Zhang, D.; Luo, H.; Zheng, L.; Wang, K.; Li, H.; Wang, Y.; Feng, H. Utilization of waste phosphogypsum to prepare hydroxyapatite nanoparticles and its application towards removal of fluoride from aqueous solution. *J. Hazard. Mater.* **2012**, *241*, 418−426.

(9) Gobbitt, J. M. Yara Hemihydrate (HH) and Hemidihydrate (HDH) Processes for Phosphoric Acid Production. *Procedia Eng.* **2012**, *46*, 143−153.

(10) Koopman, C.; Witkamp, G. J. Ion exchange extraction during continuous recrystallization of $CaSO_4$ in the phosphoric acid production process: lanthanide extraction efficiency and $CaSO_4$ particle shape. *Hydrometallurgy* **2002**, *63*, 137−147.

(11) Liu, D.; Wang, C.; Mei, X.; Zhang, C. An effective treatment method for phosphogypsum. *Environ. Sci. Pollut. Res.* **2019**, *26*, 30533−30539.

(12) Wang, C.; Liu, D.; Huang, Q. A new civil engineering material: normal temperature modified phosphogypsum embedded filler. *Arch. Civ. Mech. Eng.* **2021**, *21*, 5.

(13) Wu, P. Recrystallization process and dihydrate-hemihydrate recrystallization process. *Phosphate Fertilizer. Compound Fertilizer.* **1994**, *3*, 16−21.

(14) Xiang, S.; Wu, Y.; Fan, B. Study on a new type of hemihydrate-dihydrate wet process phosphoric acid extraction process. *S. P. Bmh. Related. Eng.* **2018**, *03*, 39−43.

(15) Singh, N. B.; Middendorf, B. Calcium sulphate hemihydrate hydration leading to gypsum crystallization. *Prog. Cryst. Growth Charact. Mater.* **2007**, *53*, 57−77.

(16) Hand, R. J. The kinetics of hydration of calcium sulphate hemihydrate: A critical comparison of the models in the literature. *Cem. Concr. Res.* **1994**, *24*, 885−895.

(17) Ridge, M. J.; Surkevicius, H. Hydration of calcium sulphate hemihydrate. I. Kinetics of the reaction. *J. Appl. Chem.* **1962**, *12*, 246−252.

(18) Freyer, D.; Voigt, W. Crystallization and Phase Stability of $CaSO_4$ and $CaSO_4$-Based Salts. *Monatsh. Chem.* **2003**, *134*, 693−719.
(19) Li, Z.; Demopoulos, G. P. Solubility of $CaSO_4$ Phases in Aqueous HCl + $CaCl_2$ Solutions from 283 to 353 K. *J. Chem. Eng. Data* **2005**, *50*, 1971−1982.
(20) Fu, H.; Jiang, G.; Wang, H.; Wu, Z.; Guan, B. Solution-Mediated Transformation Kinetics of Calcium Sulphate Dihydrate to α-Calcium Sulphate Hemihydrate in $CaCl_2$ Solution at Elevated Temperature. *Ind. Eng. Chem. Res.* **2013**, *52*, 17134−17139.
(21) Skrdla, P. J.; Robertson, R. T. Semiempirical equations for modeling solid-state kinetics based on a Maxwell-Boltzmann distribution of activation energies: Applications to a polymorphic transformation under crystallization slurry conditions and to the thermal decomposition of $AgMnO_4$ crystals. *J. Phys. Chem. B* **2005**, *109*, 10611−10619.
(22) Skrdla, P. J. Crystallizations, solid-state phase transformations and dissolution behavior explained by dispersive kinetic models based on a Maxwell-Boltzmann distribution of activation energies: theory, applications, and practical limitations. *J. Phys. Chem. A* **2009**, *113*, 9329−9336.
(23) Grzmil, B.; Kic, B.; Żurek, O.; Kubiak, K. Studies on the transformation of calcium sulphate dihydrate to hemihydrate in the wet process phosphoric acid production. *Pol. J. Chem. Technol.* **2012**, *14*, 80−87.
(24) Luo, G.; Wang, Y.; Xue, J.; Zhang, F. The actual discovery of the regular layer polytype with α=102° in chlorite. *J. N. Univ. (Nat. Sci).* **2001**, *37*, 805−808.
(25) Dumazer, G.; Narayan, V.; Smith, A.; Lemarchand, A. Modeling gypsum crystallization on a submicrometric scale. *J. Phys. Chem. C* **2009**, *113*, 1189−1195.
(26) Guan, B.; Jiang, G.; Fu, H.; Yang, L.; Wu, Z. Thermodynamic Preparation Window of Alpha Calcium Sulphate Hemihydrate From Calcium Sulphate Dihydrate in Non-Electrolyte Glycerol-Water Solution Under Mild Conditions. *Ind. Eng. Chem. Res.* **2011**, *50*, 13561−13567.
(27) Li, Z.; Demopoulos, G. P. Model-based construction of calcium sulphate phase-transition diagrams in the HCl-$CaCl_2$-H_2O system between 0 and 100 °C. *Ind. Eng. Chem. Res.* **2006**, *45*, 4517−4524.
(28) Wu, P. Hemi/dihydrate 2-step process for concentrated phosphoric acid. *Phosphoric Acid. Phosphate Fertilizer.* **2000**, *15*, 16−20.

https://dx.doi.org/10.1021/acsomega.0c05432
ACS Omega 2021, 6, 7342−7350